Chapter 3 - Second Harmonic Generation (SHG) Of Ionically Self-Assembled Monolayer (ISAM) Thin Films: Effect of Synthetic Laponite RD Platelets and Polycation Type

3.1 Abstract:

Multilayer, polymeric thin films containing second order nonlinear optically (NLO) active molecules of PCBS exhibit a strong dependence on the distance of the NLO active chromophore from the hard interface provided by the deposition substrate. Introduction of hard laponite platelets to mimic the effect of this hard interface does not reverse this trend. However, the laponite layer sustains the second harmonic signal of the multilayer films over large quadlayer numbers, which is seen to degenerate in the absence of the laponite.

3.2 Introduction:

Nonlinear optical (NLO) materials are of great interest in telecommunications, signal processing, and data storage technologies. Recently there has been much interest in the use of polymeric materials exhibiting second harmonic generation or frequency doubling for electro-optic (EO) modulators as a substitute for the current state-of-the-art inorganic materials which are expensive and difficult to manufacture. Frequency doubling occurs due to the materials ability to change its refractive index and thus altering the frequency of the light passing through it [1]. The phenomenon of frequency altering by a medium when an electric field is applied is called the Pockels effect [2]. An example of this is the conversion of the commercial infrared laser (wavelength of 1064 nm), to green light (wavelength of 532 nm), when passed through one of these second-order nonlinear media. This transformation is useful because it quadruples the amount of information the laser can write on an optical disc [3]. Materials that exhibit this frequency doubling undergo a polarization when subjected to an electric field, which at any time t, is given by

$$P(t) = \chi^{(1)} E(t) + \chi^{(2)} [E(t)]^2 + \chi^{(3)} [E(t)]^3 + \ldots\ldots \quad (1)$$

Where,

E(t) is the electric field at time t, either from incident light, or applied externally

$\chi^{(1)}$ is the linear dielectric susceptibility

$\chi^{(2)}$, $\chi^{(3)}$ are the higher order nonlinear susceptibilities.

When $\chi^{(2)}$ and higher order terms are zero, the material is said to be linear whereas a nonlinear material has non-zero higher order susceptibilities. The specific class of nonlinear materials that is discussed in this study is the second-order nonlinear materials or the ones that have a non-zero $\chi^{(2)}$, which can only be obtained from nonlinear noncentrosymmetric materials. In nonlinear centrosymmetric materials, due to the constraint of inversion symmetry, $\chi^{(2)}$ has to be zero since they exhibit a zero time-averaged polarization. Figure 1 shows the different polarization responses to the applied field. Nonlinear noncentrosymmetric media have a finite time-averaged polarization (Figure 1d). A nonlinear optical response requires a material with a preferred orientation at both the microscopic and macroscopic level. These materials have applications in the field of opto-electronic devices. For a thin, organic film comprised of NLO-active chromophores, $\chi^{(2)}$ can be written as

$$\chi^{(2)} = NF\beta\langle\cos^3\theta\rangle \quad (2)$$

where,

N is the number of NLO active molecules,

F is the local field correction factor,

β is the hyperpolarizability of the chromophore used and

$\langle\cos^3\theta\rangle$ is the average cosine$^3\theta$, where

θ is the angle of molecular orientation of the chromophore as shown in Figure 2.

The hyperpolarizability, β, is an intrinsic property of the chromophore and can be measured experimentally with the electric field induced SHG (EFISH) method for

chromophores with no ionic groups and with the Hyper Rayleigh Scattering (HRS) for the chromophores with ionic groups attached [4].

Most of the materials that are currently used in electro-optic modulators are inorganic single crystals such as lithium niobate, potassium dihydrogen phosphate and β-barium borate [5]. The $\chi^{(2)}$ exhibited by these materials range from 1-100 x 10^{-9} esu, which is comparable to the one obtained from quartz (1.53 x 10^{-9} esu). However, fabrication of these single crystals is a complicated process requiring conditions of high pressures and temperatures [5]. Incorporation of these crystals into commercial devices is also a difficult procedure [3]. Some other disadvantages of these crystals are that they have a large mass, high cost, poor environmental stability, and also undergo deterioration due to atmospheric humidity. All these limitations associated with the inorganic crystals have led to the quest for better electro-optic materials, among which organic polymers show the most promise. For EO applications, organic NLO optical materials have three distinct advantages over their inorganic counterparts [6]. One is the low dielectric constants characteristic of organic (polymeric) materials. A low dielectric constant reduces the resistor-capacitor (RC) delay time constant and therefore increases the speed of the device. The second is the relatively constant refractive index of organic EO polymers for wavelengths from infrared to microwave region and thus ensures proper modulator operation over that range. Thirdly, polymeric materials offer the advantage of ease of manufacture and of integration with semiconductor electronics [7].

In order for new polymeric materials to be useful for EO applications, they must possess large nonlinear coefficients, good thermal, temporal and mechanical stability as well as ease of processing. These materials should be easily integrated into optical devices that are compatible with fiber optics, have low power consumption, and operate at higher frequencies [8]. Some of the advantages offered by polymeric materials are due to the fact that they can be prepared in fiber and thin-film forms, they offer low optical loss, and are significantly cheaper than their inorganic counterparts.

There are several techniques that are used for fabricating inorganic noncentrosymmetric films that exhibit SHG. One of these is the deposition of preformed monolayers from a gas-liquid interface to a solid planar substrate called the Langmuir-Blodgett (LB) deposition [9-10]. However, there are several disadvantages involved with this method. One of them is that it can only be used for molecules that are water-insoluble and have surfactant-like properties. Also, the resultant films are held together by Van der Waals forces and hence have poor thermal and mechanical stability. Covalent self-assembly of molecular adsorbates onto solid substrates involves covalent bonds between the monolayers and is used to overcome the instability problems associated with the LB films [11]. However, covalent self-assembly is a tedious process and requires suitable control of reaction conditions. It is also a time consuming process and is limited in the choice of materials. This is because certain reactions may require deposition conditions of high temperatures and pressures and thus can be expensive. It is also limited by the extent of reaction for each of the assembly processes. Thus although this method boasts of high optical constants, has several limitations that has prevented this method to become very commercially popular.

Another technique used for applications of polymer films in nonlinear optical applications is that of poled polymers. In this method NLO polymers are poled by applying an electric field [12]. Typically a polymer containing NLO chromophores is first spin-coated on a conducting substrate forming films that are about a micron thick [13]. Subsequently, the film is heated to its glass transition temperature, where in its rubbery state, it is exposed to a strong static electric field, so that the chromophores are aligned to achieve the necessary noncentrosymmetry. Then the polymer is cooled to room temperature in the presence of the field to freeze the alignment. The electric field is then removed, and the restricted mobility below the glass transition temperature of the polymers preserves the chromophore orientation even in the absence of the electric field. Two common methods of electric field poling are corona-poling or contact electrode poling [12]. An alternative to covalently attaching the chromophore to the polymer is to dope the chromophore into an optically inactive polymer and then the mixture is deposited on the surface. This is called a guest-host system. As seen by the processing, it is obvious that materials that can be used for this technique must have a high glass

transition temperature. This is because, to be useful for device applications, the nonlinear response should be stable during device processing and fabrication, which may involve elevated temperatures exceeding 100-150 °C, even for a period of minutes. Materials that have a low glass transition may lose orientation during the fabrication processes involving elevated temperatures. The stability of these films could further deteriorate if the chromophore acts as a plasticizer and reduces the glass transition temperature. Thus, despite the high SHG exhibited by these films, the disadvantages associated with them limits their effectiveness.

The technique used in this study for constructing multilayer thin films is ionic self-assembly [14]. In this, polymers are adsorbed onto charged substrates in a self-limiting manner and the monolayers are stably held together by ionic interactions and possibly hydrogen bonding interactions. Ionically self-assembled monolayer (ISAM) films can be used for a variety of thin film applications since they are easy to fabricate, inexpensive in comparison with some of the alternative methods and can be controlled easily by simple changes in solution pH and ionic strength. Another extremely important advantage these films have is that they deposit within just a few minutes as compared to the time-consuming and high temperature conditions sometimes associated with some of the alternative methods. McAloney et al [15] have shown that the initial polymer adsorption occurs in less that 10 seconds. In our own study for all polymeric systems, the maximum deposition time has been not more that 5 minutes. Thus within a matter of hours, a multilayer film can be prepared with relative ease. For a similar number of layers, other techniques can take as much as a few days.

Recently there has been considerable interest in the NLO properties of ISAM films. The orientation of the chromophore deposited in the film is the key issue that governs the magnitude of the SHG signal exhibited by these films. Lenahan et al [16] and Heflin et al [17-19] have used commercially available polymeric dyes such as a linear polydye Poly S-119, in ISAM films that exhibit SHG. Since the orientation of the chromophore in the film is not directly controlled, moderate amount of molecular scale order has been achieved thus far with maximum tilt angles of the chromophores going upto 39°. Hammond [20] suggests the attachment of rigid side groups to the main chain

of the NLO-active polymers to enhance the tendency of the chromophores to align with respect to each other due to confinement effects. The actual orientation of the chromophore in the film or the tilt angle of the chromophore can be measured experimentally. As seen from equation (2), the closer this angle is to zero degrees, the higher the $\chi^{(2)}$. One of the reasons that good control over the tilt angles is limited, is that the polymers in two-component multilayers are not stratified into well-defined layers but are dispersed and interpenetrating.

This interpenetration is felt the least in the layers close to the solid substrate. The number of initial layers required for the loss of the substrate effect depends on the polymers used, the deposition conditions such as solution pH, and the type and charge of the substrate. Beyond the initial bilayers, the polymers in adjacent layers tend to interpenetrate. Rubner and associates [21-23] worked with a number of polymers to estimate the interpenetration of adjacent polymeric layers. In one such study involving poly (p-phenylene) and poly (phenylene vinylene), they estimated that the effect of the substrate was lost after about 6 bilayers as increased interpenetration of the bilayers was seen after these initial layers. In other ISAM work done by Laschewsky and Wischerhoff [24] with NLO-active ionene-type polycation and montmorillonite and poly(vinyl sulfate) as the anionic layers, the SHG decreased after the first bilayer. Lvov et al [25] saw the SHG decrease with PDDA/PCBS films in 4 bilayers. We hypothesized that introduction of impenetrable clay platelets of laponite will limit the degree of interpenetration and hence provide better control over chromophore orientation. Glinel et al [26] have studied the deposition of laponite with polycations of varying structures, and the best deposition results in terms of film roughness (flattest tile-like laponite deposition) were obtained with PDDA as the polycation. They also show that laponite increases the order in the multilayers formed with each of the polycations and prevent interpenetration of the different polymer layers.

This chapter is the second of a two-part study that is aimed at using ionically self-assembled monolayer (ISAM) thin films containing a synthetic hectorite, laponite for electro-optic modulators. In Chapter 2, it was demonstrated that ordered multilayer films with regular layer-by-layer growth (using ellipsometry and UV/Vis spectroscopy)

containing laponite, a polycation PDDA and an NLO-active chromophore, PCBS can be constructed. In this chapter, we investigate the second-order nonlinear optical properties of these films. The main idea of this two-part study is to counter the problem of interpenetration of monolayers in ISAM films in order to achieve better control of the NLO-active chromophore and hence enhance the second harmonic generation of these films.

As mentioned earlier, ISAM films in electro-optic modulators should have a high $\chi^{(2)}$, which requires orientation of the chromophore in the film. One of the problems for achieving better control on the orientation and also increasing the tilt angle of the chromophore is the interpenetration of the monolayers in the film and the loss of the effect of the solid substrate. Several studies have confirmed that two-component multilayers are not stratified into well-defined layers but are dispersed and interpenetrating [27-29]. Our hypothesis is that if we introduce a layer in these films that mimics the effect of a solid substrate, we may be able to optimize the orientation. For this purpose we chose to use of a synthetic hectorite called Laponite RD. Laponite is a purely synthetic hectorite-type clay. The deposited platelets are nanometer size with a thickness of about one nanometer. This is a water-dispersible clay that deposits negatively charged platelets of about 35 nm on positively charged surfaces. The first work with clays and ISAM films was done by Kleinfeld and Ferguson [30-32] where they used the electrostatic layer-by-layer adsorption of oppositely charged components to produce ultrathin ceramic/polycation multilayers. A variety of clays have been studied for this, but the majority of the work with ISAM films has been done with montmorillonite [33] and laponite.

Laponite platelets are usually stacked into aggregates, in which clay sheets are separated by exchangeable cations and one or two water layers [34]. Each layer comprises three sheets, two outer tetrahedral silica sheets and a central octahedral magnesium sheet. Part of the magnesium in the central sheet is replaced by lithium, resulting in a net negative charge of the layer, which is balanced by sodium ions located between adjacent layers in a stack [35]. The presence of these smectite particles in the films generates a number of interesting properties such as stabilization of the layered structure and adsorption of active molecules (e.g. electroactive, photoactive). Unlike

other inorganic materials, laponite in film has the capability to “heal” packing defects formed in the preceding adsorption cycle.

Another reason for choosing Laponite was the reported smoothness of ISAM films made with it compared to those made with other clays. There is a variety of natural and synthetic clays that could be used. Suspensions of natural colloidal clay platelets exhibit a wide variety of structural and mechanical properties and are frequently used as thickeners, fillers and antisettling agents [36]. Montmorillonite is one such natural clay which deposits as single sheets or thin platelets composed of 2-3 sheets in which the negative charge is balanced by inter and intra-lamellar sodium cations [37]. These platelets are about 200 nm in size. The disadvantage that natural clays have when compared with their synthetic counterparts is that they are usually very polydisperse in both shape and size. Synthetic clays comparatively have a much higher degree of monodispersity when in solution. Van duffel et al [38] compared ISAM film formation using laponite and a natural hectorite as the anionic species and PDDA as the polycation. Films formed by natural clays were found to be significantly rougher than films made with synthetic clays. This was believed due to either the overlapping of natural clay particles more with each other as compared to the synthetic clays when adsorbed on positively charged surfaces or possibly a lesser extent of adsorbtion as compared to synthetic clays.

In the first part of the study the layer-by-layer growth of these thin films was monitored with ellipsometry and UV/Vis spectroscopy for up to 25 quadlayers, each comprising of two layers of the polycation and one layer each of the polymeric dye and laponite with the sequence of polycation-laponite-polycation-dye. AFM images of the terminal laponite layer show flat tile-like deposition of laponite platelets that are about 25-35 nm in diameter. The introduction of platelets of this size into ISAM films in a flat, tile-like manner, would then approximate the effect of the charged glass substrate and thus serve to orient the chromophores.

We have also compared the effect of a hard vs soft interface on the SHG signal of ISAM films by creating a soft interface of NLO-inactive polymer bilayers before the

deposition of the chromophore. To study the effect of a hard vs a soft interface, we conducted experiments with varying number of spacer layers between the chromophore containing layer and the hard glass interface. Films with 0, 1, 2, 5, 7, 10 spacer layers and a terminating polycation-chromophore layer were made and compared with a film with 5 spacer layers and a laponite containing chromophore layer to check if laponite can mimic the effect of a hard interface.

3.3 Experimental

Materials

The materials used for this work include two polycations, an NLO-active polymeric dye, an NLO-inactive polyanion, and Laponite RD clay. Deionized water was obtained from a NanoPure II system with a resistivity of 18 Ω-cm. Reagent grade NaOH, HCl, H_2O_2, NH_4OH, and phosphoric acid were used.

The polycations used in this work were poly(diallyldimethylammonium chloride) or PDDA [Sigma-Aldrich; 100,000 < Mw < 200,000 g/mole; "low molecular weight" received as a 20 wt% solution in water; repeat unit molecular weight of 161 g/mole] and poly(allylamine hydrochloride) or PAH [Polysciences; Mw ~ 70,000 g/mole; repeat unit molecular weight of 92 g/mole]. The structure of PAH is shown in Figure 3b. The structure of the polycation is shown in Figure 3. Poly{1-[4-(3-carboxy-4-hydroxyphenylazo)benzenesulfonamido]-1,2-ethanediyl, sodium salt} or PCBS [Sigma-Aldrich; MW ~ 100,000 g/mole; repeat unit molecular weight of 371 g/mole] was the polyanionic dye used for this study. Another anionic polymer used was the sodium salt of poly(acrylic acid) (PAA) [Polysciences Inc; MW~ 5000; repeat unit molecular weight of 94 g/mole]. The structures of the two polyanions are shown in Figures 4a and 4b. All of these polymers were used as received.

The clay used for this study was Laponite RD [Southern Clay Products, Texas], a synthetic hectorite-type clay with a density of 2570 Kg/m^3, a surface area of 900 m^2/g [39], and a mean chemical composition: SiO_2 66.2 %, MgO 30.2 %, Na_2O 2.9 %, and Li_2O 0.7 % [40]. When properly dispersed, Laponite has a reported high degree of monodispersity, which should facilitate flatter deposition. The idealized chemical

formula for Laponite RD is given by $[(Si_8(Mg_{5.34}Li_{0.66})O_{20}(OH)_4]Na_{0.66}$. The cation exchange capacity (CEC) of laponite platelets is 0.95 meq/g. The primary platelets dimensions are 0.97 nm thick and a diameter ~ 25-35 nm. A more complete description of Laponite is given in Chapter 2. Dispersion conditions are discussed in more detail in the Results section below.

Solution and Suspension Preparation

Stock solutions of polymers and laponite were prepared by mixing in a beaker with about 80% of the final volume of water and the solutions were stirred for about 1 hour. The remaining amounts of water were then added and the solutions were typically stirred overnight. The pH was then adjusted to the desired value with NaOH or HCl.

Slide Cleaning

Glass microscope slides obtained from Fischer Scientific were used as substrates for the films. The slides were prepared for dipping using the RCA cleaning method given below. In the RCA cleaning method, glass is cleaned using two solutions – a base and an acid solution. The base solution was composed of 92.6 ml H_2O, 10.3 ml H_2O_2 (30% w/w), 17.2 ml NH_4OH mixed in a volumetric flask - the mixture was swirled for 30 sec after the addition of each component. The acid solution was composed of 96.0 ml H_2O, 9.0 ml H_2O_2, 15.0 ml HCl (1.18M) mixed in a volumetric flask - the mixture was swirled for 30 sec after the addition of each component.

Glass slides were put in a glass-slide holder, base solution was added, the holder was covered with a lid and placed in a dish filled with DI water. This assembly was then placed on a heating plate. After the temperature reached 70 °C, it was left for 20 min and then the slides were removed. The slides were then rinsed with the rising procedure mentioned above and placed in a clean glass-slide holder, after which the acid solution added. After 20 min, they were removed and rinsed again. These were then put in another glass-slide holder and placed uncovered in the oven at 130 °C, for at least an hour. Then they were removed from the oven and allowed to cool. The slides were now ready for dipping. The slides treated in this manner are negatively charged for deposition of the first monolayer of the polycation, which was positively charged.

Film Formation Procedure

Dipping conditions.

For both polycations, the concentration used in the dipping experiments was 0.01 mole repeat unit/liter and the dipping time was 5 minutes. The polycations were deposited at pH 7 and 10 although most of the work was done at a pH 7. The PCBS was deposited at pH 7 in all cases and the dipping time was 5 minutes. The concentration of the PCBS was 0.01 mole repeat unit/liter and was deposited at pH 7 in all cases with a dipping time of 5 minutes. The concentration of PAA was 0.01 mole repeat unit/liter and was deposited at a pH of 4.5 in all cases with a dipping time of 5 minutes.

The Laponite RD was deposited at a concentration of 0.2 % w/w in DI water where the unadjusted pH was approximately 10. This condition was determined by dynamic light scattering experiments, described earlier in Chapter 2, to give individual platelets with equivalent spherical hydrodynamic diameters of 25-35 nm. The dipping time for the laponite suspensions was 5 minutes in all cases.

Dipping was done in standard dipping jars with about 40 ml of the solutions. First, the charged glass slide was dipped into the polycation solution (PDDA or PAH) and was then rinsed thoroughly with DI water. The rinsed slide was then dipped into the polyanionic PCBS solution.

Rinsing between the dipping steps was done with DI water. After removal from the dipping jar, each slide was first agitated in a 40 ml beaker containing DI water for about 5 sec to remove loosely bound polymer and then 500 ml of DI water was poured over it for further rinsing. This procedure was repeated twice.

Drying of slides.

Slides were dried in a stream of nitrogen gas filtered through a 5 micron filter. Drying was done usually every 5 bilayers/quadlayers, and at the end of the final bilayer/quadlayer deposition. It was also done after the deposition of every laponite layer.

Deposition sequence.

A polycation layer was first deposited on a cleaned, negatively charged glass slide. This was followed by a layer of Laponite clay and was then followed by another

layer of the polycation and then the PCBS dye. This constitutes a quadlayer and is illustrated in Figure 4a. This sequence was then repeated to deposit more quadlayers.

For the spacer experiments with poly (acrylic acid) (PAA), each of the spacer layers comprised of PDDA and PAA. After the deposition of the desired spacer layers a terminal bilayer of PDDA and NLO dye was deposited. Figure 4b shows deposition sequence for a two-spacer layers experiment.

Film Characterization

Details of characterization of the films made with PDDA, Laponite, and PCBS were detailed earlier in Chapter 2 and so a summary of the results is presented here. Layer-by-layer growth of the films was established characterized by measuring the absorbance at 359 nm of films after the deposition of every 5 quadlayers and by measuring the film thickness with ellipsometry. Atomic force microscopy (AFM) images of the films' surfaces established that the Laponite layers deposited in a flat, tile-like manner.

SHG Measurements

Measurements of are made through the use of a Nd: YAG – pumped optical parametric oscillator. The laser source is a Q-switched Nd: YAG 10 Hz pulsed laser with a 15 ns pulse width. The fundamental wavelength is 1064 nm (infrared), with a fundamental pulse energy of 500 mJ. A photodiode and a photomultiplier tube collect reference and SHG signal data, respectively. Data is collected and processed by a CAMAC crate interfaced with a PC, where it is analyzed with the combination of a home-written code, PSI–Plot v4.56 (Poly Software International) and Tablecurve v3.0 (Jandel Scientific)[17-19]. The error in the SHG measurements is $\pm$ 10 %.

3.4 Results

In the first part of the study of NLO-active clay-ISAM nanocomposites in Chapter 2, we demonstrated that regular, layer-by-layer growth occurred for films comprised of quadlayers with the deposition sequence PDDA-Laponite-PDDA-PCBS. Table 1 summarizes the results from that study. Figure 6 shows that the square root of the SHG signal generated from these films after normalization based on the absorbance of the PCBS chromophore - increased by about 30 % as the quadlayer number varied from 10 to 50. This normalization takes into account the variation in deposition of PCBS from slide to slide that can greatly affect the reproducibility of the SHG response. The number of quadlayer deposition cycles was between 5 and 25, but the generated signal came from film on both sides of the substrate and hence the total number of quadlayers on both sides of the substrate varied between 10 and 50. Unless otherwise noted, the reported SHG data were normalized on the absorbance of the PCBS chromophore and will have the format of $[\text{SHG}/(\text{Absorbance of PCBS})^2]^{1/2}$.

The absorbance-adjusted SHG response of the films comprised of bilayers made with PDDA/PCBS with spacer layers of PDDA/PAA is shown in Figure 7. The square root of the SHG signal dropped by about 50% upon the insertion of a PAA/PDDA spacer layer and remained effectively constant thereafter up to 10 spacer layers. For another film series made at the same conditions, shown in Figure 8A, the square root of the absorbance-adjusted SHG signal dropped by a factor of 10 as the spacer layer number ranged from 0 to 5. Figure 8A also shows that the presence of a Laponite-containing layer capped with a terminal layer of PCBS/PDDA after 5 spacer layers of PDDA/PAA has no effect on the square root of the SHG signal. Figure 8B shows the raw SHG data not normalized for the PCBS absorbance. It is important to note that the absorbance of all the different was not the same indicating that the amount of chromophore deposited in each case was different. To compare these results obtained with PDDA, we performed similar experiments with the polycation, poly(allylamine hydrochloride) or PAH. Figures 10 and 11A and 11B with PAH are analogous to Figures 7 and 8A and 8B with PDDA.

3.5 Discussion

Laponite/PDDA/PCBS films

To successfully use these films for commercial second-order NLO applications, the bulk SHG has to scale quadratically with the number of layers deposited [17-19]. As seen in Figure 6, the laponite containing films do not demonstrate this effect. However the trend seen in Figure 6 is different from NLO behavior observed by Guzy et al [41] for films made with PDDA / PCBS and no laponite as shown in Figure 9. As seen in Figure 9, there seems to be no discernable trend for the PDDA (pH 7) / PCBS films, and the bulk SHG signal drops when the pH of the polycation is increased to 10. In comparison, our study shows that the presence of laponite, maintains or maybe even slightly increases the bulk signal over increasing number of quadlayers, although the growth is not the desired quadratic increase of SHG with number of layers. As mentioned earlier, in work done with PDDA/PCBS by Lvov et al [25], the SHG decreased in about 4 bilayers. In view of the results obtained these groups and our data, we hypothesize that although laponite does not contribute to the bulk SHG signal, it does contribute in limiting the interpenetration of the adjacent bilayers, resulting in maintaining the bulk SHG at higher quadlayer numbers. This also indicates that the presence of a hard interface significantly affects the SHG signal.

PDDA/PAA/PCBS spacer experiments

Figure 7 shows that the square root of the absorbance-adjusted SHG signal drops sharply as the NLO active PCBS layer is moved further away from the hard interface in the films made without Laponite. All of the drop in the signal is seen right after the insertion of the first spacer layer and remains approximately constant after that. This is consistent with results from earlier work [21-23,25] showing that the effect of the interface decays after 4-6 bilayers away from the interface. Figure 8A clearly indicates that the drop in the normalized SHG is not reversed for films with Laponite and a terminating PDDA/PCBS bilayer, and hence these hard Laponite platelets do not mimic the strong effect of the hard glass interface. The possible movement of the Laponite platelets in the films during deposition could be the reason for this effect. This problem could be solved if these platelets could be bound covalently to the adhering surface,

restricting their in-film movement and thus enhancing their ability to form an impenetrable surface. One could also try depositing solid layers of pure silica by reactive deposition using silicon alkoxides such as tetraethyl orthosilicate, which, under controlled conditions of pH and temperature, can result in the deposition of reasonably pure layers of silica.

PAH/PAA/PCBS spacer experiments

For films made with PAH as the polycation instead of PDDA, the trends for the raw and absorbance-adjusted data are different from those with PDDA. Comparing Figure 10 for films made with PAH to Figure 7 for films made with PDDA, the drop in the square root of the absorbance-adjusted SHG signal for films made with PAH is not as abrupt. The average of the normalized SHG signal for films with spacer layer numbers ranging from 0-2 is almost twice as high as the average for films with spacer layer numbers ranging from 5-10. The effect of a laponite-containing layer shown in Figure 11A led to a 50% reduction in the normalized SHG signal, which is different for films with PDDA shown in Figure 8A where the SHG response did not change with the insertion of the laponite-containing layer.

In the work done by Guzy et al [41], films made with the two polycations at the same deposition conditions (pH 7) and at the same time had similar SHG signals for the first bilayers deposited with PCBS. Combining their results with the results of this study, it shows that interpenetration of bilayers potentially leading to a decrease in SHG is a more likely phenomenon with PDDA as the polycation. This can be confirmed with the spacer layer experiment, which indicates that, for PDDA, the drop in SHG is seen with 1 spacer layer, whereas with PAH the drop is more pronounced after the deposition of 2 spacer layers. In either case, however the effect of the impenetrable glass substrate on the SHG is lost after the deposition of the first few layers. The introduction of laponite does not reverse this trend. The laponite platelets seem to further disturb the order for the films containing PAH. From results obtained in the previous chapter and previous work done with laponite by other groups, the presence of quarternary amine groups in PDDA promotes the organized deposition of laponite. Future studies need to be conducted to

establish the relationship between film formation and type of polycation used with laponite.

3.6 Conclusions

This two-part study has thus shown that although Laponite-polymer composite films with an NLO-active dye can be successfully made with good control and reproducibility, and the introduction of the hard platelets limits the interpenetration of the adjacent layers to some extent, quadratic growth of bulk SHG was not exhibited by these films due to the absence of a hard glass interface at each layer. This is confirmed by the comparison of depositing a single NLO-active bilayer on hard as well as a soft interface, emphasizing again the importance of a hard interface for enhanced second harmonic generation signals.

3.7 Acknowledgements

- This work was supported by grant # ECS-9907747 from the National Science Foundation.
- Charles Brands and Patrick Neyman for SHG measurements

3.8 References

[1] "Electro-optic Effects and Optically Nonlinear materials", W. Du, www.phys.vt.edu/~graupner/5555/Du/sld001.htm, 1999.

[2] R. W. Boyd, "Nonlinear Optics", Academic Press, Rochester, New York, 1992.

[3] "Devices Based on Electro-optic Polymers Begin To Enter Marketplace", Ron Dagani, *Chemical & Engineering News, March 4,22-27,* 1996.

[4] H. S. Nalwa, S. Miyata, "Nonlinear Optics of Organic Molecules and Polymers", CRC Press, Boca Raton, 1997.

[5] "Potassium titanyl phosphate: properties and new applications", J. D. Bierlein, H. Vanherzeele, *J. Opt. Soc. Am. B, 6, No.4, 622-633,* 1989.

[6] "Electroactive polymers including non-linear optical polymers", A. Ren, L. R.

Dalton, *Curr. Opin. Coll. Interface Sci., 4, 165-171,* 1999.

[7] "Polymeric electro-optic modulators: From chromophore design to integration with semiconductor VLSI electronics and silica fiber optics", L.R. Dalton, A.W. Harper, J. Chen, S. Mao, S. Sun, C. Zhang, M. He, *Ind. Eng. Chem. Res., 38, 8-33,* 1999.

[8] D. Bloor, "Conjugated and non-segmented polymers in integrated optics", 23-34, IOP Publishing Ltd., 1990.

[9] A. Ulman, "An Introduction to Ultrathin Organic Films: From Langmuir-Blodgett to Self-Assembly", Academic Press, Boston, MA, 1991.

[10] G. L. Gaines Jr., "Insoluble Monolayers at Liquid-Gas Interfaces", Interscience, New York, 1966.

[11] "Adsorption of ordered zirconium phosphonate multilayer films on silicon and gold surfaces", H. Lee, L. Kepley, H. Hong, S. Akhter, T. Mallouk, *J. Phys. Chem., 92, 2597-2601,* 1988.

[12] "Second-order nonlinearity in poled polymer systems", D.M. Burland, R.D. Miller, C.A. Walsh, *Chem. Rev., 94, 3-29,* 1994.

[13] "Second-order non-linear optical polymers", C. Samyn, T. Verbiest, A. Persoons, *Macromol. Rapid Commun., 21, 1-15,* 2000.

[14] "Buildup of ultrathin multilayer films by a self-assembly process: III. Consecutively alternating adsorption of anionic and cationic polyelectrolytes on charged surfaces", G. Decher, J. D. Hong, J. Schmitt, *Thin Solid Films 210/211, 831-835,* 1992.

[15] "In Situ Investigations of Polyelectrolyte Film Formation by Second Harmonic Generation", R.A. McAloney, M.C. Goh, *J. of Phys. Chem. B, 103, 10729-10732,* 1999.

[16] "Novel Polymer Dyes for Nonlinear Optical Applications Using Ionic Self-Assembled Monolayer Technology", K. Lenahan, Y. Wang, Y. Liu, *Adv. Mater., 10, 853-855,* 1998.

[17] "Noncentrosymmetric Ionically Self-Assembled Thin Films for Second Order Nonlinear Optics", J. R. Heflin, Y. Liu, C. Figura, D. Marciu, R. Claus, *Organic Thin Films for Photonics Applications, v 14, 78-80,* 1997.

[18] "Second Order Nonlinear Optical Thin Films Fabricated from Ionically Self-Assembled Monolayers", J. R. Heflin, Y. Liu, C. Figura, D. Marciu, R. Claus, *Proc.*

SPIE, 3147, 10-19, 1997.

[19] "Thickness Dependence of Second-Harmonic Generation in Thin Films Fabricated from Ionically Self-assembled Monolayers", J. R. Heflin, C. Figura, Y. Liu, D. Marciu, R. Claus, *Appl. Phys. Lett., 74, 495-497,* 1999.

[20] "Recent explorations in electrostatic multilayer thin film assembly", P. Hammond, *Curr. Opin. Coll. & Interface Sci., 4, 430-442,* 2000.

[21] "Controlling Bilayer Composition and Surface Wettability of Sequentially Adsorbed Multilayers of Weak Polyelectrolytes", D. Yoo, S. Shiratori, M. Rubner, *Macromolecules, 31, 4309-4318,* 1998.

[22] "Forster Energy Transfer Studies of Polyelectrolyte Heterostructures Containing Conjugated Polymers: A Means To Estimate Layer Interpenetration", J. Baur, M. Rubner, J. Reynolds, S. Kim, *Langmuir, 15, 6460-6469,* 1999.

[23] "pH-Dependent Thickness Behavior of Sequentially Adsorbed Layers of Weak Polyelectrolytes", S. Shiratori, M. Rubner, *Macromolecules, 33, 4213-4219,* 2000.

[24] "Polyelectrolyte Multilayer Assemblies Containing Nonlinear Optical Dyes", A. Laschewsky, E. Wischerhoff, *Macromolecules, 30, No.26, 8304-8309,* 1997.

[25] "Non-linear optical effects in layer-by-layer alternate films of polycations and an azobenzene-containing polyanion", Y. Lvov, S. Yamada, T. Kunitake, *Thin Solid Films, 300, 107-112,* 1997.

[26] "Ordered Polyelectrolyte "Multilayers". 3. Complexing with Clay Platelets with Polycations of Varying Structure", K. Glinel, A. Laschewsky, A. M. Jonas, *Macromolecules, 34, 5267-5274,* 2001.

[27] "Fuzzy Nanoassemblies Toward Layered Polymeric Multicomposites", G. Decher, *Science, 277, 1232-1237,* 1997.

[28] "Detailed Structure of Molecularity Thin Polyelectrolyte Multilayer Films on Solid Substrates as revealed by Neutron Reflectometry", M. Losche, J. Schmitt, G. Decher, W. G. Bouwman, K. Kjaer, *Macromolecules, 31, 8893-8906,* 1998.

[29] "Internal structure of layer-by-layer adsorbed polyelectrolyte films: a neutron and x- ray reflective study", J. Schmitt, T. Grunewald, G. Decher, P. S. Pershan, K. Kjaer, M. Losche, *Macromolecules, 26, 7058-7063,* 1993.

[30] "Stepwise Formation of Multilayered Nanostructural Films from Macromolecular

Precursors", E. R. Kleinfeld, G. S. Ferguson, *Science, 265, 370-373*, 1994.

[31] "Rapid, Reversible Sorption of Water from the Vapor by a Multilayered Composite Film: A Nanostructured Humidity Sensor", E. R. Kleinfeld, G. S. Ferguson, *Chem. Mater., 7, 2327-2331*, 1995.

[32] "Mosaic Tiling in Molecular Dimensions", E. R. Kleinfeld, G. S. Ferguson, *Adv. Mater., 7, 414-416*, 1995.

[33] "Formation of Ultrathin Multilayer and Hydrated Gel from Montmorillonite and Linear Polycations", Y. Lvov, K. Ariga, I. Ichinose, T. Kunitake, *Langmuir, 12, 3038-3044*, 1995.

[34] "Fuzzy Assembly and Second Harmonic Generation of Clay/Polymer/Dye Monolayer Films", B. van Duffel, T. Verbiest, S. V. Elshocht, A. Persoons, F. C. De Schryver, R. A. Schoonheydt, *Langmuir, 17, 1243-1249*, 2001.

[35] "Unusual Thixotropic Properties of Aqueous Dispersions of Laponite RD", N. Willenbacher, *J. Colloid Interface Sci., 182, 501-510*, 1996.

[36] "Sol-Gel Transitions in Aqueous Suspensions of Synthetic Takovites. The Role of Hydration Properties and Anisotropy", L. J. Michot, J. Ghanbaja, V. Tirtaatmadja, P. J. Scales, *Langmuir, 17, 2100-2105*, 2001.

[37] "Mechanism of and Defect Formation in the Self-Assembly of Polymeric Polycation – Montmorrilonite Ultrathin Films", N. A. Kotov, T. Haraszti, L. Turi, G. Zavala, R. E. Geer, I. Dekany, J. H. Fendler, *J. Am. Chem. Soc., 119, 6821-6832*, 1997.

[38] "Multilayered Clay Films: Atomic Force Microscopy Study and Modelling", B. van Duffel, R. A. Schoonheydt, *Langmuir, 15, 7520-7529*, 1999.

[39] Technical Directory for Laponite, Laporte Industries Ltd., UK.

[40] "Structure of gels and aggregates of disk-like colloids", T. Nicolai, S. Cocard, *Eur. Phys. J. E 5, 221-227*, 2001.

[41] "Polar Orientation of an Anionic Chromophore Side Group in Ionically Self-Assembled Films: Effect of Polycation pH and Structure", M. Guzy et al. (Manuscript in preparation).

3.9 Tables & Figures

Table I – Absorbance and Thickness per quadlayer

PDDA pH	Absorbance*/Quadlayer	$\sigma_{absorbance}$	Thickness/Quadlayer (nm)	$\sigma_{thickness}$ (nm)
7	0.00186	0.00015	1.8	0.1
10	0.0032	0.00014	2.8	0.2

*measured at 359 nm

(Note: Standard deviation (σ) was calculated using least squares regression [63]).

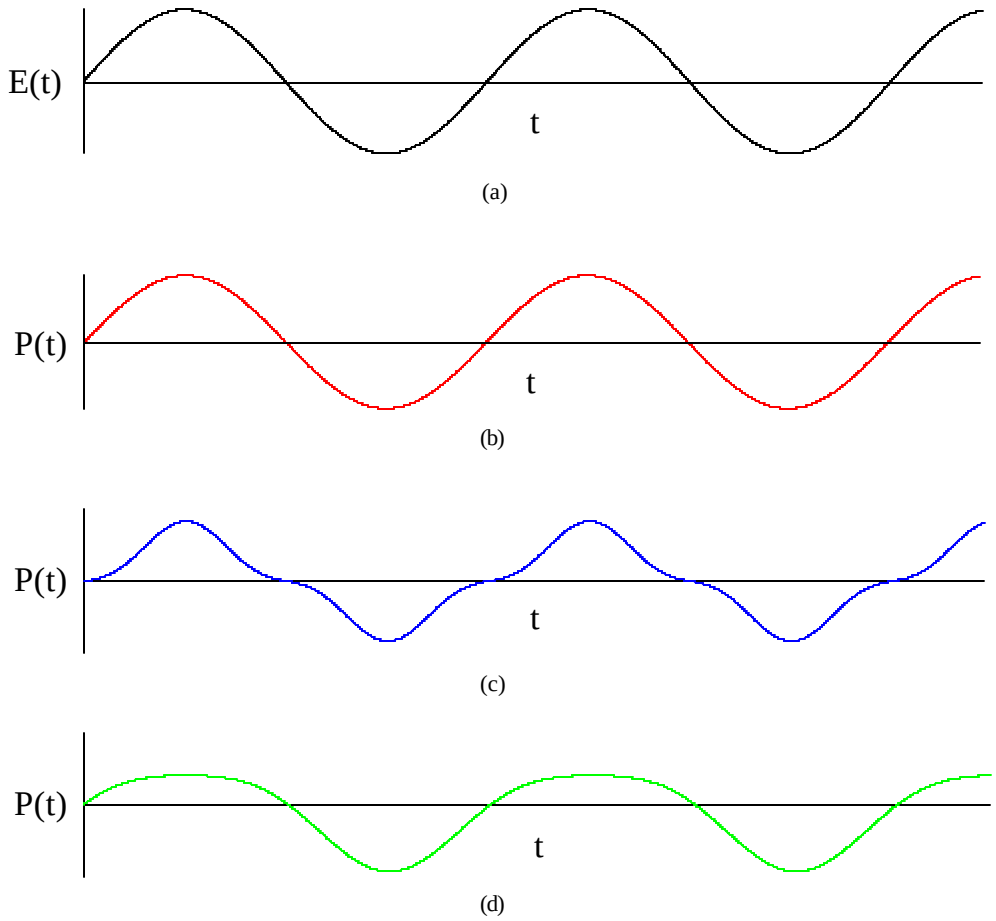

Figure 1. Electric field and corresponding polarization fields in various media. (a) Incident electric field. (b) Polarization field of (a) in linear, centrosymmetric medium. (c) Polarization field of (a) in centrosymmetric, nonlinear medium. (d) Polarization field of (a) in noncentrosymmetric, nonlinear medium. Only (d) has non-zero time-averaged polarization field (and non-zero $c^{(2)}$)

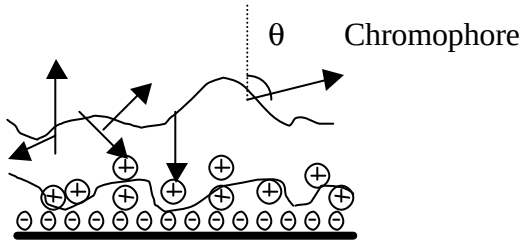

Figure 2. Molecular orientation angle – It is the angle that the chromophore makes with the axis normal to the substrate.

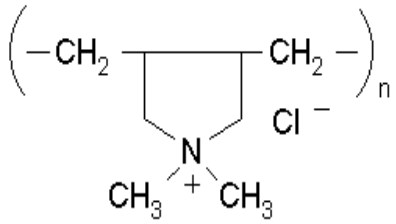

Figure 3a. Structure of the polycation used: PDDA

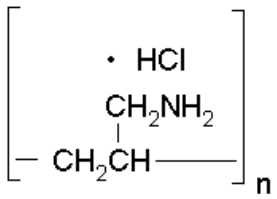

Figure 3b. Structure of the polycation used: PAH

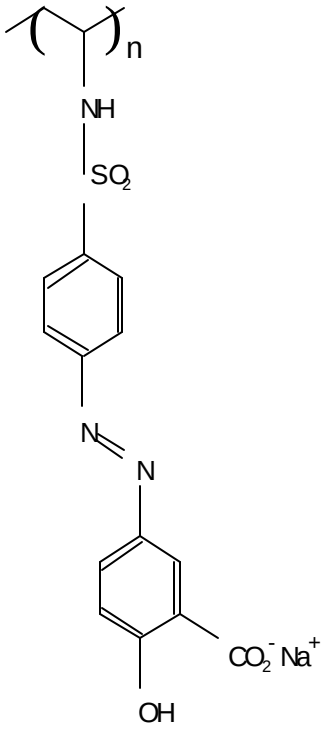

Figure 4a. Structure of PCBS

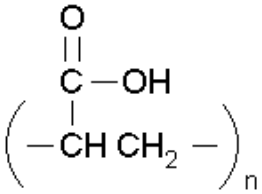

Figure 4b. Structure of Poly (acrylic acid)

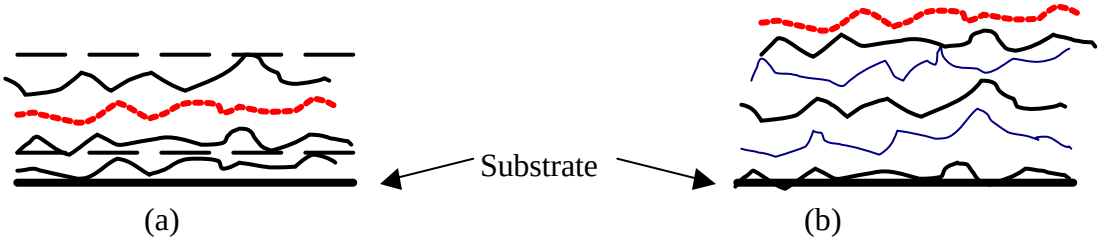

Figure 5. Deposition sequence (a) with laponite every quadlayer (b) with a chromophore after two spacer layers. Polycation, Chromophore, Laponite, and PAA.

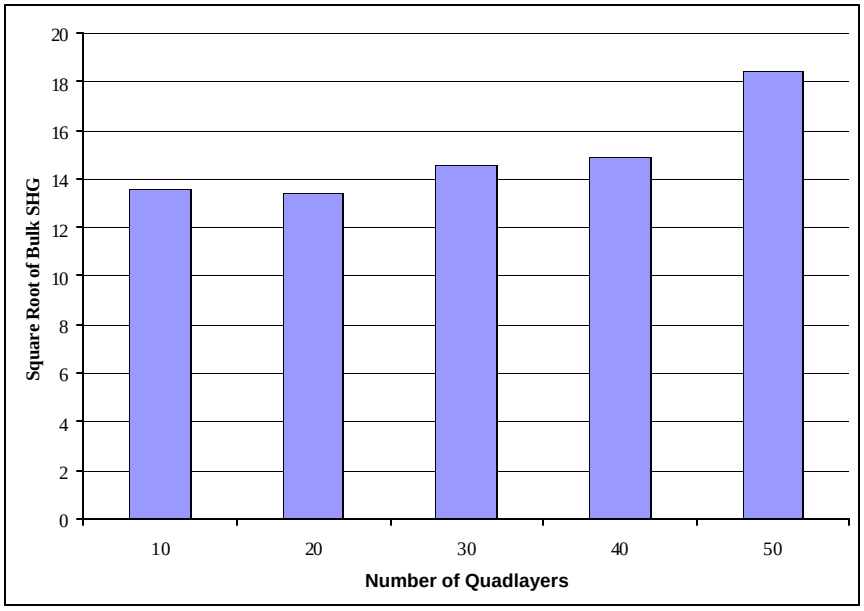

Figure 6. Bulk SHG signal as a function of number of quadlayers for 10, 15, 20, 40 and 50 quadlayer (polycation-laponite-polycation-chromophore) films with PDDA (pH 7) / Laponite (pH 10) / PCBS (pH 7). Data shown are an average of series 18 and 34. (Note: Number of quadlayers on the film is twice the number of deposition cycles, considering there is film deposited on both sides of the glass slide)

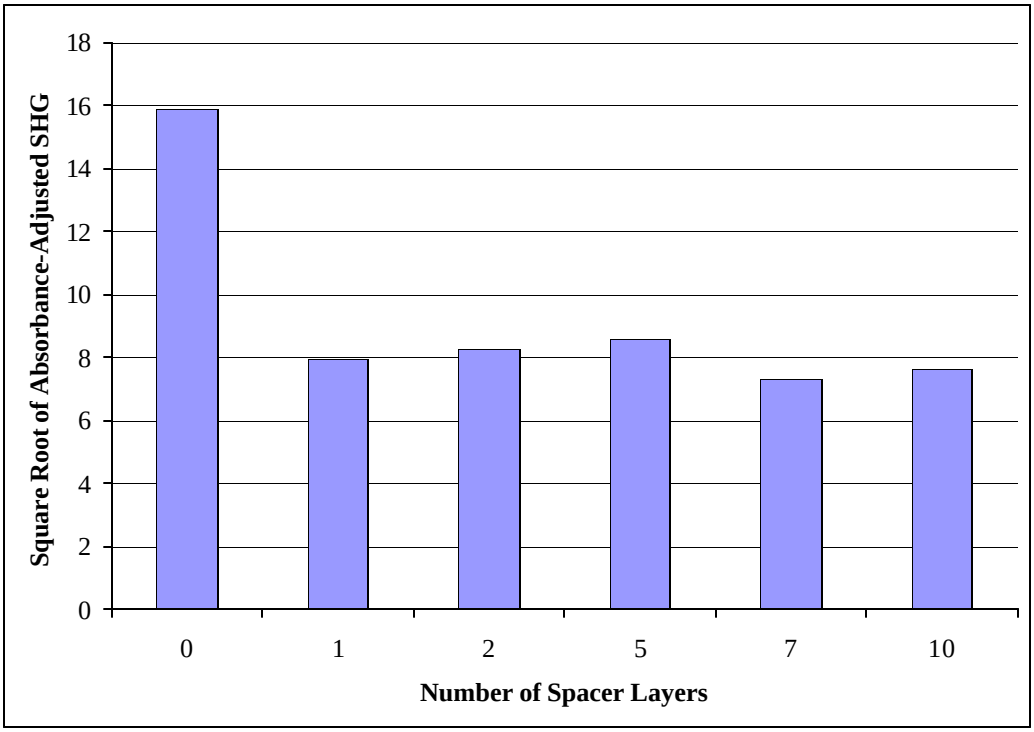

Figure 7. Absorbance-adjusted bulk SHG data of films with a terminating bilayer of PDDA (pH 7) / PCBS (pH 7) and with different number of spacer layers. Spacer layers are bilayers of PDDA (pH 7) / PAA (pH 4.5). Data shown are an average from series 38 and 40.

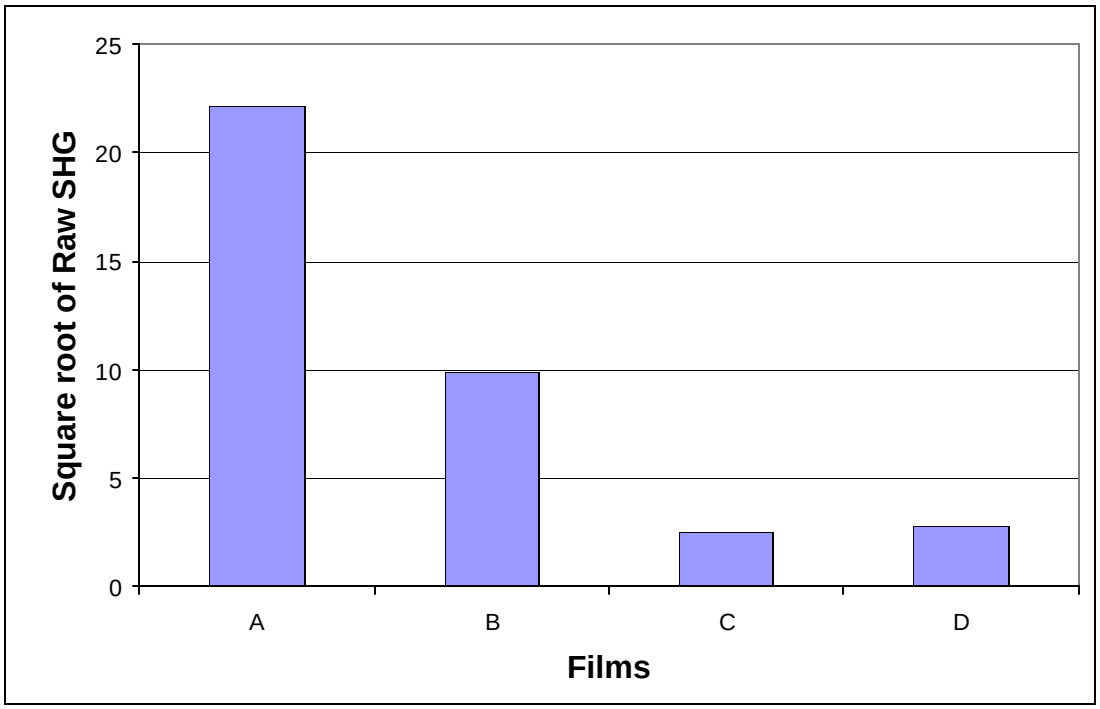

Figure 8A. Absorbance-adjusted bulk SHG data of films with a terminating bilayer of PDDA (pH 7) / PCBS (pH 7) and – A: no spacer layers, B: 2 spacer layers, C: 5 spacer layers, D: 5 spacer layers and a bilayer of PDDA (pH 7) / Laponite (pH 10). Spacer layers are bilayers of PDDA (pH 7) / PAA (pH 4.5). Data shown are from series 28.

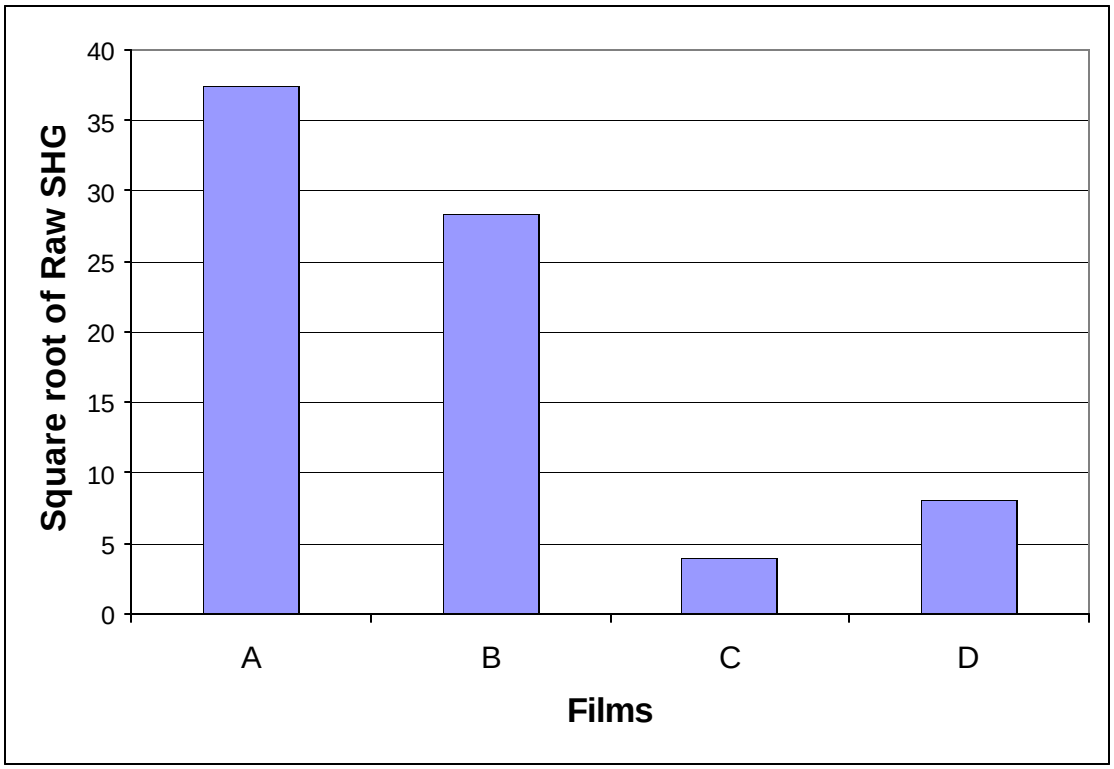

Figure 8B. Raw bulk SHG data of films with a terminating bilayer of PDDA (pH 7) / PCBS (pH 7) and – A: no spacer layers, B: 2 spacer layers, C: 5 spacer layers, D: 5 spacer layers and a bilayer of PDDA (pH 7) / Laponite (pH 10). Spacer layers are bilayers of PDDA (pH 7) / PAA (pH 4.5). Data shown are from series 28.

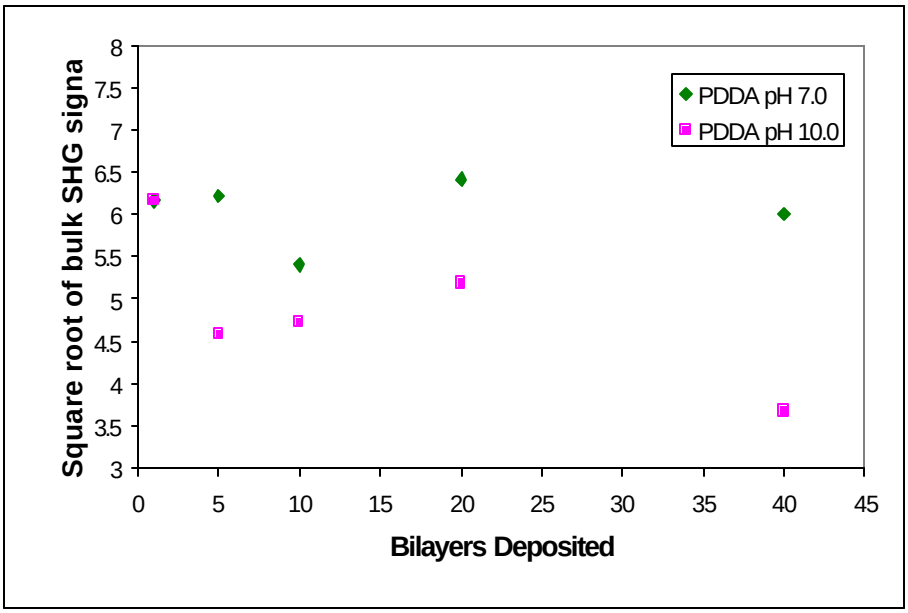

Figure 9- Nonquadratic scaling of SHG intensity with the number of PDDA/PCBS bilayers deposited for different PDDA pH [41].

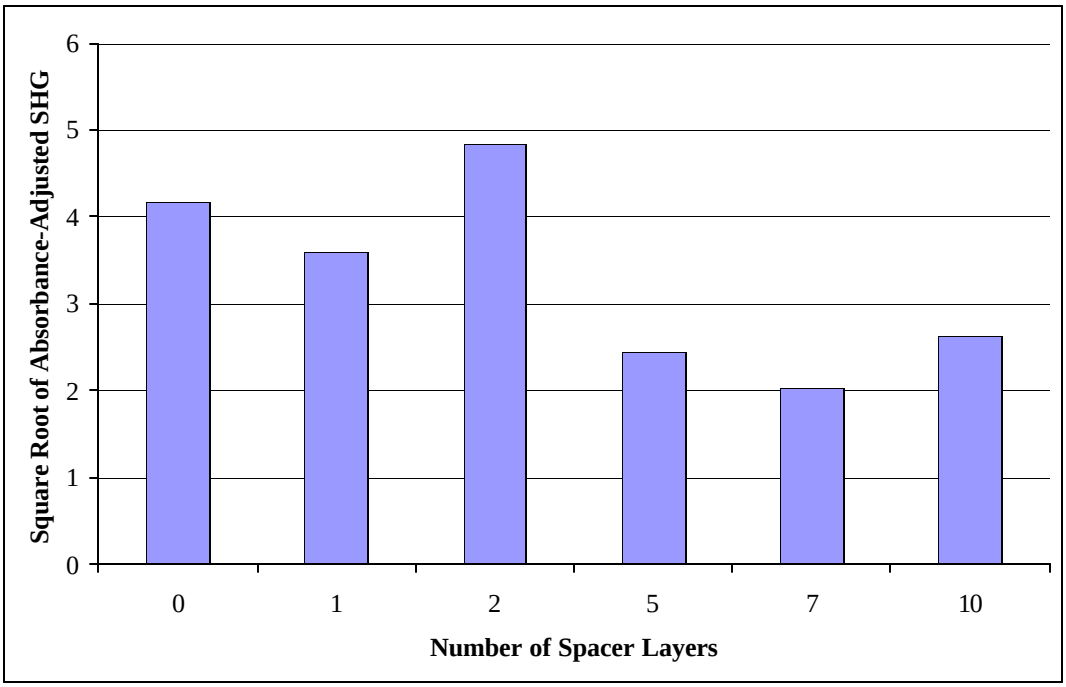

Figure 10. Absorbance-adjusted bulk SHG data of films with a terminating bilayer of PAH (pH 7) / PCBS (pH 7) and with different number of spacer layers. Spacer layers are bilayers of PAH (pH 7) / PAA (pH 4.5). Data shown are an average of series 39 and 41.

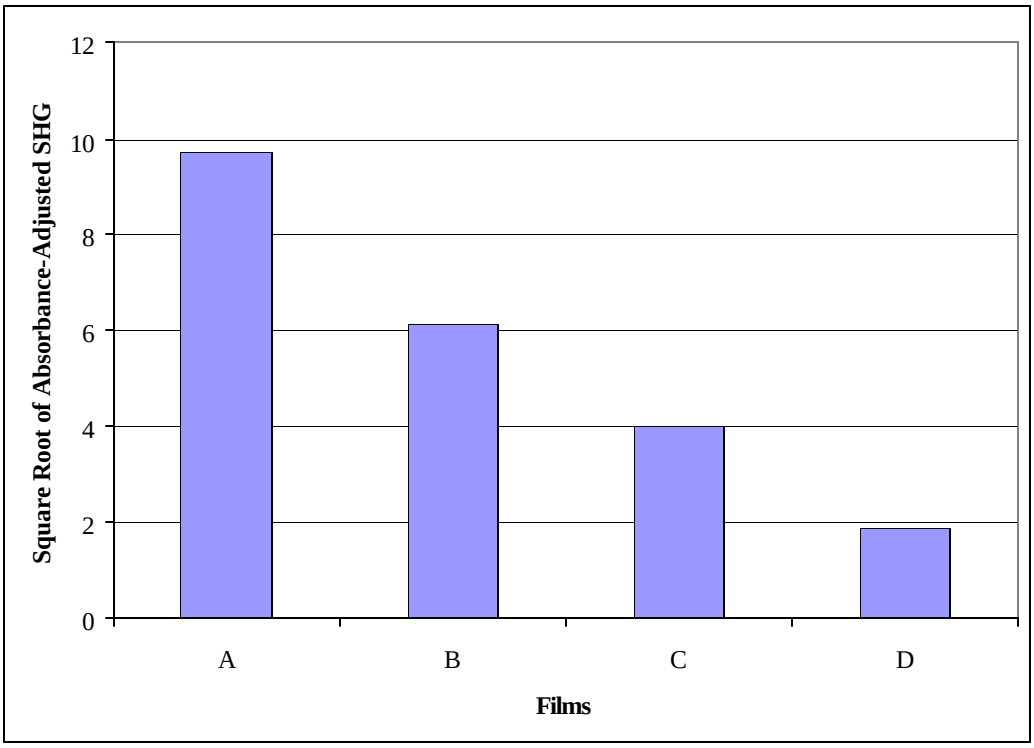

Figure 11A. Absorbance-adjusted bulk SHG data of films with a terminating bilayer of PAH (pH 7) / PCBS (pH 7) and – A: no spacer layers, B: 2 spacer layers, C: 5 spacer layers, D: 5 spacer layers and a bilayer of PAH (pH 7) / Laponite (pH 10). Spacer layers are bilayers of PAH (pH 7) / PAA (pH 4.5). Data shown are from series 27.

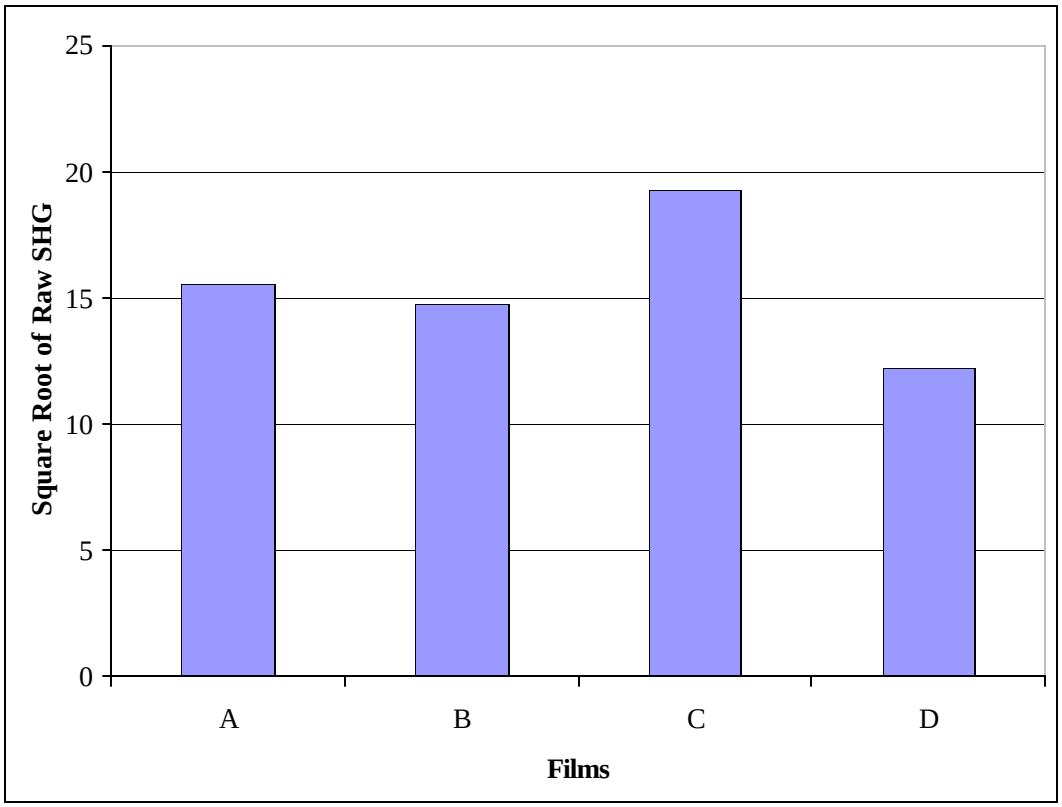

Figure 11B. Raw bulk SHG data of films with a terminating bilayer of PAH (pH 7) / PCBS (pH 7) and – A: no spacer layers, B: 2 spacer layers, C: 5 spacer layers, D: 5 spacer layers and a bilayer of PAH (pH 7) / Laponite (pH 10). Spacer layers are bilayers of PAH (pH 7) / PAA (pH 4.5). Data shown are from series 27.